

Article

Relationships between Microstructural Parameters and Time-Dependent Mechanical Properties of a New Nickel-Based Superalloy AD730™

Louis Thebaud ^{1,2,*}, Patrick Villechaise ^{2,†}, Jonathan Cormier ^{2,†}, Coraline Crozet ¹, Alexandre Devaux ¹, Denis Béchet ¹, Jean-Michel Franchet ³, Antoine Organista ⁴ and Florence Hamon ²

¹ Aubert & Duval, Site des Ancizes, Research and Development Department, BP1, 63770 Les Ancizes Cedex, France; E-Mails: coraline.crozet@eramet-aubertduval.com (C.C.); alexandre.devaux@eramet-aubertduval.com (A.D.); denis.bechet@eramet-aubertduval.com (D.B.)

² Institut Pprime, UPR CNRS 3346, Physics and Mechanisc of Materials Department, ISAE-ENSMA, 1 Avenue Clément Ader, BP 40109, 86961 Futuroscope-Chasseneuil, France; E-Mails: patrick.villechaise@ensma.fr (P.V.); jonathan.cormier@ensma.fr (J.C.); florence.hamon@ensma.fr (F.H.)

³ Safran SA, SafranTech—Materials & Process Division, Rue des Jeunes Bois—Châteaufort—CS 80112, 78772 Magny-Les-Hameaux, France; E-Mail: jean-michel.franchet@safran.fr

⁴ Safran Turbomeca, Avenue Joseph Szydlowski, 64511 Bordes, France; E-Mail: antoine.organista@turbomeca.fr

† These authors contributed equally to this work.

* Author to whom correspondence should be addressed; E-Mail: louis.thebaud@cnrs.pprime.fr; Tel.: +33-5-49-49-83-67 (ext. 33); Fax: +33-5-49-49-82-38.

Academic Editor: Johan Moverare

Received: 5 November 2015 / Accepted: 23 November 2015 / Published: 27 November 2015

Abstract: High temperature creep and dwell-fatigue properties of the new nickel-based superalloy AD730™ have been investigated. Three microstructures have been studied in creep (850 °C and 700 °C) and dwell-fatigue (700 °C stress control with trapezoidal signals, and dwell times ranging from 1 s to 3600 s): a coarse grains microstructure, a fine grains one, and single crystalline samples. The aim of this study is to assess the influence of the grain size on creep and creep-fatigue properties. It is demonstrated that fine and coarse grains microstructures perform similarly in creep at 700 °C, showing that the creep properties at

this temperature are controlled by the intragranular precipitation. Moreover, both the coarse grains and the fine grains microstructures show changes in creep deformation mechanisms depending on the applied stress in creep at 700 °C. At higher creep temperatures, the coarse grains microstructure performs better and almost no effect is observed by suppressing grain boundaries. During dwell-fatigue tests at 700 °C, a clear effect of the mechanical cycling has been evidenced on the time to failure on both the coarse and the fine grains microstructures. At high applied stresses, a beneficial effect of the cyclic unloading to the lifetime has been observed whereas at lower applied stresses, mechanical cycling is detrimental compared to the pure creep lifetime due to the development of a fatigue damage. Complex creep-fatigue interactions are hence clearly evidenced and they depend on the pure creep behavior reference.

Keywords: cast and wrought Ni-based superalloy; single crystals; creep; dwell-fatigue properties; high temperatures; creep threshold stress; inter/intra granular properties

1. Introduction

Increasing aero-engine efficiency and reducing NO_x emissions is generally achieved in gas turbines by increasing the operating temperatures. Precipitate strengthened nickel-based superalloys, which are mainly used for the rotating parts of the hottest sections of such aero engines, have to be able to withstand higher temperatures to meet these requirements. For instance, the objective of original engine makers is to reach operating temperatures above 700 °C in the rim sections of high pressure turbine disks, a temperature range at which state of the art superalloys such as Alloy 718 cannot be used anymore [1,2]. AD730™ is a new nickel-based superalloy, developed by Aubert & Duval for turbine disks or seal ring applications, with the particularity of being less expensive than its direct challengers due to its chemical composition and its good workability, enabling it to be manufactured through the cast and wrought route [3–6].

During service operations, such high temperature components are subjected to several mechanical solicitations, already widely studied, such as creep and fatigue. However, complex interactions take place between these two classical loading types [7–10], suggesting that the study of each one separately is not sufficient. In an aim to achieve more representative conditions, one would prefer to use dwell-fatigue tests to mimic real operation conditions of high-pressure turbine disks (e.g., take off, cruise, and landing).

In this context, the aim of this paper is to study the mechanical properties of this alloy under creep and dwell-fatigue loading conditions. These properties are highly dependent on microstructural parameters, such as grain size, grain boundary morphology, and the size and the morphology of the strengthening phase γ' [11]. In this study, a special focus will be paid to the influence of the grain size on these properties.

2. Experimental Procedure

2.1. Material

Two polycrystalline microstructures and one single crystalline microstructure have been studied, all coming from the same ingot of AD730™ provided by Aubert & Duval (Les Ancizes, France), having the chemical composition given in Table 1. The polycrystalline material was supplied by Aubert & Duval, as an 87 mm forged bar. Blanks were cut along the longitudinal direction, at mid-radius, prior to heat treatment. Two kinds of microstructures were studied. The first one, improved for creep resistance, presents a homogeneous coarse grains distribution, with an average grain size of about 350 μm . The second one is a fine grains microstructure, developed for high tensile strength, low cycle fatigue, and disk burst resistance (average grain size: 10 μm). These microstructures will be denoted in the following article as “coarse grains” (CG) and “fine grains” (FG) microstructures, respectively. The coarse grains microstructure was obtained by a supersolvus heat treatment composed of two solution treatments: 2 h at 1120 $^{\circ}\text{C}/70$ $^{\circ}\text{C min}^{-1}$ + 4 h/1080 $^{\circ}\text{C}/\text{Air Quench (AQ)}$ followed by a two-step aging: 4 h/800 $^{\circ}\text{C}/\text{AQ}$ + 16 h/760 $^{\circ}\text{C}/\text{AQ}$, while the fine grains microstructure was obtained by one solution treatment followed by one aging: 4 h/1080 $^{\circ}\text{C}/\text{AQ}$ + 8 h/730 $^{\circ}\text{C}/\text{AQ}$ [6].

Table 1. Chemical composition (in wt. %) of AD730™ nickel-based superalloy.

| Element | Ni | C | Cr | Mo | W | Al | Co | Ti | Nb | Fe | B | Zr |
|---------|---------|-------|----|----|-----|-----|-----|-----|-----|----|------|------|
| Wt. % | Balance | <0.02 | 16 | 3 | 2.7 | 2.3 | 8.5 | 3.5 | 1.1 | 4 | 0.01 | 0.03 |

A third microstructure was used for this study: single crystalline (SX) bars made of AD730™ were casted by SNECMA-SAFRAN Group (Gennevilliers, France). These bars were casted along a $\sim[001]$ crystallographic orientation. The same supersolvus heat treatment as the coarse grains microstructure has been performed on these single crystals in order to be able to compare the grain size with the same precipitation distribution.

Microstructural observations performed using a JEOL 7000F field emissions gun scanning electron microscope (FEG-SEM) are shown in Figure 1. The microstructural characteristics of these three microstructures are presented in Table 2.

Table 2. Characteristics of the three microstructures (N.O. = Not Observed).

| Microstructure | Grain Size | Average γ' Precipitation Size | | | |
|-----------------|-------------------|--------------------------------------|------------------|--------------------------|----------|
| | | Primary | Coarse Secondary | Fine Spherical Secondary | Tertiary |
| Fine Grains | 10 μm | 1 μm | X | 40 nm | N.O. |
| Coarse Grains | 350 μm | X | 300 nm | 35 nm | N.O. |
| Single Crystals | X | X | 300 nm | 35 nm | N.O. |

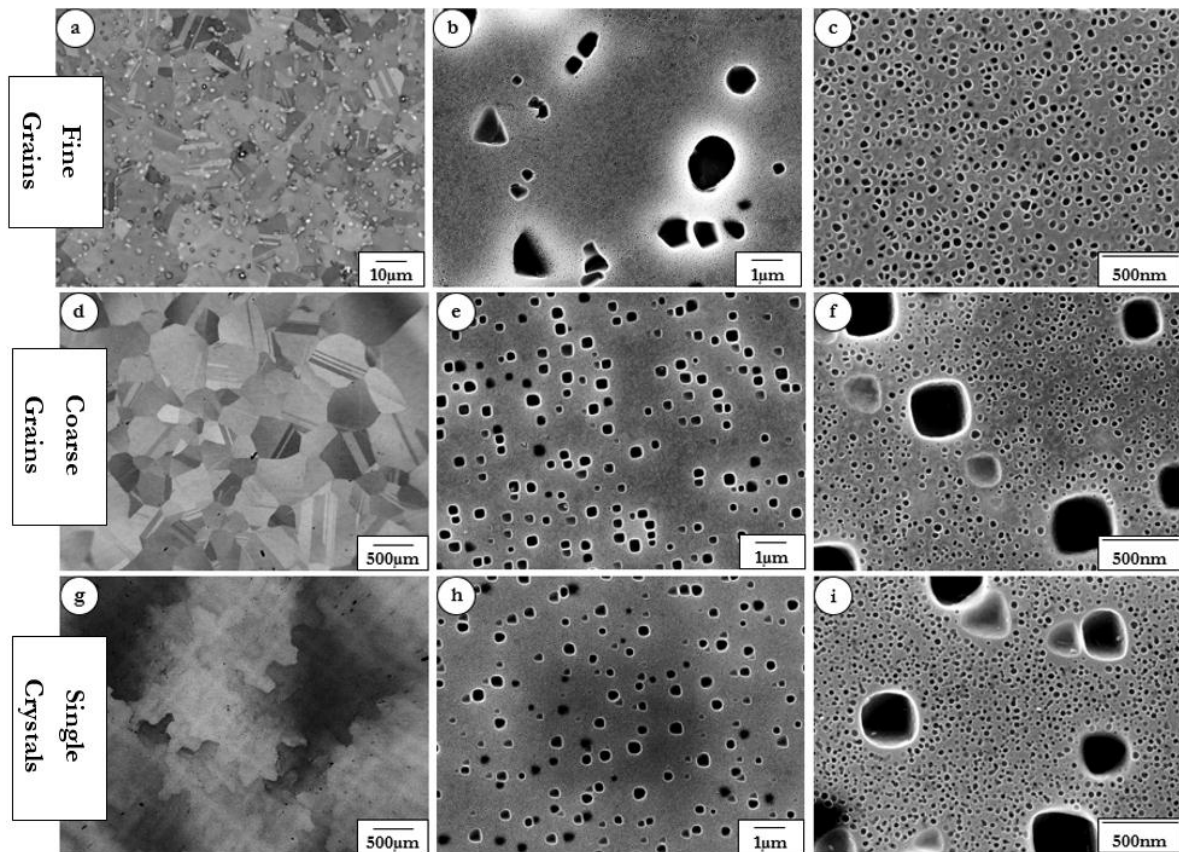


Figure 1. Granular microstructure observed in SEM back-scattered electron mode (**a, d, g**), and coarse and fine γ' precipitation (**b, e, h** and **c, f, i** respectively) observed using the secondary electron mode for the fine grains microstructure (**a, b, c**), coarse grains microstructure (**d, e, f**) and the single crystals microstructure (**g, h, i**). Note that boundaries observed in (**g**) correspond to low angle boundaries (crystallographic misorientation less than three degrees between each domain).

The fine grains microstructure is composed of primary γ' with an average size of about 1 μm , and fine secondary γ' (~ 40 nm diameter), while both the coarse grains and the single crystals exhibit a bimodal distribution of secondary γ' precipitates, with coarse cuboidal γ' particles having a ~ 300 nm size and fine spherical γ' with an average diameter of about 35 nm.

2.2. Mechanical Testing

Mechanical tests on FG and CG samples were performed on cylindrical specimens having a 13 mm gauge length, and a 4.3 mm diameter. SX samples, only tested in creep, have a 14 mm gauge length and a 4 mm diameter.

Before mechanical testing, samples were polished with SiC papers up to a 4000 grade for creep testing under air. For all the other mechanical solicitations, additional polishing with diamond sprays was performed up to a 1 μm grade.

Pure creep tests were conducted in tension with a constant load. Elongation was continuously monitored using a Linear Variable Displacement Transducer (LVDT: Solartron Metrology, Bognor Regis, UK).

Creep tests under vacuum were done with an Instron 1271 type hydromechanical machine (Instron France, Elancourt, France).

Dwell-fatigue tests were conducted under air at 700 °C with an INSTRON 8862 type electromechanical machine (Instron France, Elancourt, France). These tests were performed under a stress controlled mode with trapezoidal signals, with a stress ratio $R_\sigma = 0.05$. Previous studies [7,10,12,13] have shown that depending on the hold periods (Δt) at maximum applied stress, the material durability is governed either by pure fatigue damage or pure creep damage. It was thus decided to cover a wide range of hold periods (from 1 s to 3600 s), in order to meet both criteria. The maximum applied stresses, ranging from 750 MPa to 950 MPa for the creep-fatigue tests, have been chosen in order to approximate industrial applications. Specimen elongation measurements were performed using a high temperature extensometer.

3. Results

3.1. Creep Behavior

First, creep-rupture tests were performed on these three microstructures at 850 °C. At this extreme temperature for this kind of alloy, oxidation and microstructure overageing are supposed to have a strong impact on creep properties [11]. Comparisons of the creep behaviors of the three microstructures at 850 °C are shown in Figure 2.

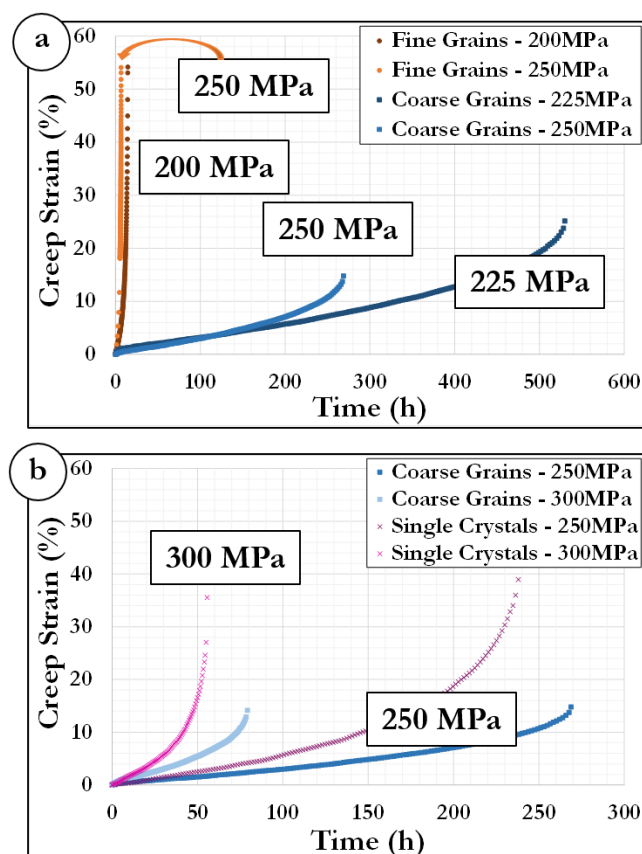


Figure 2. Creep test results at 850 °C: (a) Comparison between coarse grains and fine grains, (b) Comparison between coarse grains and single crystals.

When comparing the fine grains and the coarse grains microstructures, it is confirmed that, as expected [11], the coarse grains microstructure is more creep resistant than the fine grains one (Figure 2a), in terms of creep life, elongation, and minimum creep strain rate. Thus the grain size seems to be the main factor controlling the creep life.

One way to confirm this trend is to conduct creep tests in the same conditions, on single crystals, previously heat treated in order to have the same γ' precipitation microstructure as we have on the coarse grains microstructure (Figure 1). The results of these tests are presented in Figure 2b. This plot shows that, in this range of stress (250 MPa and 300 MPa), single crystals do not perform better than the CG polycrystalline samples (neither in term of creep life nor in creep strain rate (see later). This result suggests that there is a grain size threshold, above which the grain size is no longer the main factor controlling creep behavior. Above this grain size, the intragranular γ' volume fraction becomes the main creep controlling parameter, according to Reed [11].

The impact of oxidation was also evaluated by performing creep tests under vacuum (Figure 3). It can be seen that for both microstructures, the creep life under vacuum is about 1.5 times higher than under air, except for the creep tests performed on the fine grains microstructure at 850 °C/250 MPa. The very low time to failure (14 h) can explain this: for such a short test, oxidation did not have enough time to affect the creep properties.

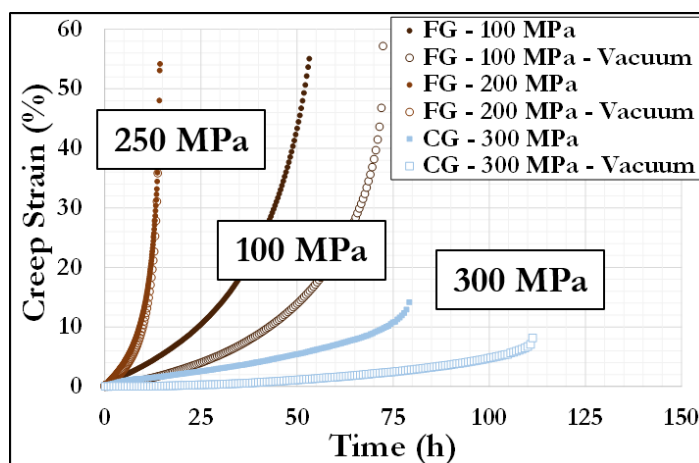


Figure 3. Comparison between creep tests performed under air and vacuum at 850 °C.

Even though the alloy's microstructural stability enables it to be used at higher temperatures (hence the coarse grains microstructure), AD730™ was initially designed to withstand temperatures up to 750 °C [3–5]. In order to get closer to such a temperature range and to assess the creep properties of this alloy in a wide range of temperatures, creep tests at 700 °C were conducted. Creep properties of both the fine grains and the coarse grains microstructures were investigated at this temperature, in the following range of stresses: 600 MPa to 850 MPa (Figure 4a).

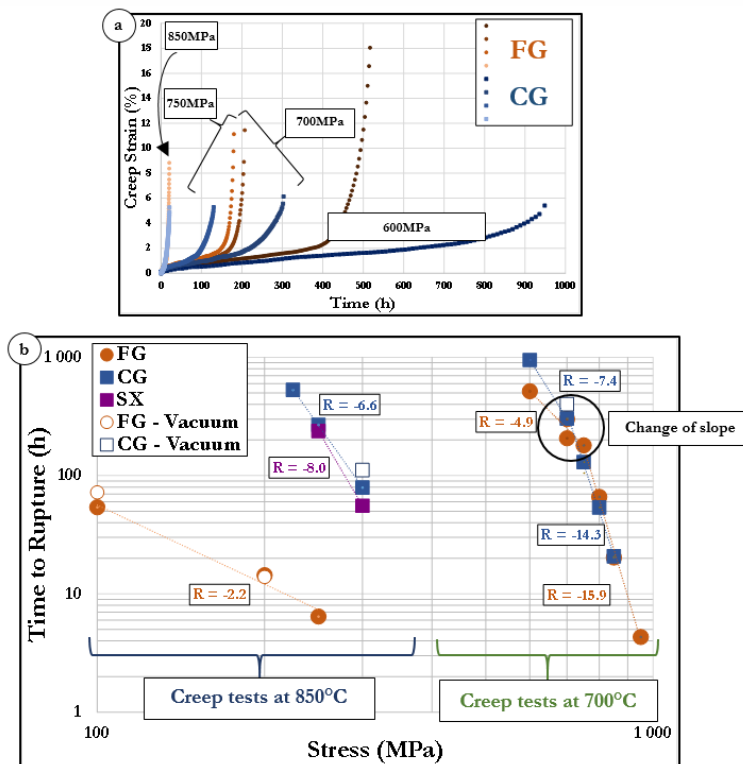


Figure 4. (a) Creep behavior at 700 °C for coarse grains and fine grains microstructures; (b) Time to rupture as a function of the applied stress.

It can be seen that, surprisingly, when the applied stress is in the range 700–850 MPa, both microstructures present very similar creep properties (creep life and creep strain rate). This suggests that the grain size has almost no impact on the creep properties in a wide range of applied stresses at 700 °C.

However, when the applied stress decreases, the coarse grains microstructure becomes more creep resistant than the fine grains one, as it does at higher temperatures. This indicates the presence of a threshold stress at which there is a change in creep deformation mechanisms and/or damage processes for at least one of the microstructures. These results are confirmed when looking at the evolution of the time to rupture, plotted as a function of the applied stress (Figure 4b) where a change of slope is observed around 750 MPa.

3.2. Dwell-Fatigue Behavior

To get closer to the service operation of turbine disks, dwell-fatigue tests have been conducted on both the fine grains and the coarse grains microstructures. This part of the study focuses more specifically on the influence of the mechanical cycling frequency compared to pure creep, and on the creep-fatigue interactions in terms of durability.

The creep-fatigue properties of the coarse grains microstructure were investigated at 700 °C, with various hold times and two maximum applied stresses: $\sigma_{max} = 750$ MPa and $\sigma_{max} = 850$ MPa (Figure 5a,b, respectively). When looking at the shapes of the curves, it appears that two separated behaviors can be evidenced. For hold times smaller than 10 s, the curves are close to pure fatigue ones, with very limited cyclic ratcheting for more than 90% of the test duration. At the end of the test, a rapid

increase of the plastic strain is observed, corresponding to the development of at least one main fatal crack.

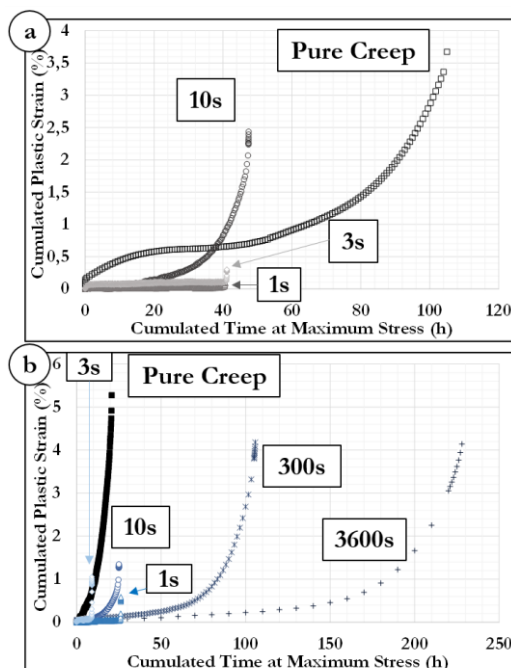


Figure 5. Plastic strain evolution during dwell-fatigue tests for different hold periods for the coarse grains microstructure: (a) $\sigma_{max} = 750$ MPa, (b) $\sigma_{max} = 850$ MPa at 700 °C.

When the hold time is longer than 10 s, the apparent mechanical behaviors are closer to pure creep ones: the three creep stages (primary, secondary, and tertiary) can be seen, and the cumulated plastic strain is higher. These results are in agreement with the results of previous studies on creep-fatigue interactions about the dependence of the viscoplastic properties to the hold time [9,10,12].

SEM fractographic observations confirm this change in mechanical behavior as a function of the applied stress. In Figure 6a, one can see a typical pure fatigue fracture surface, with a crack initiation at twin boundaries, and fatigue rivers, whereas the fracture surface shown in Figure 6b, corresponding to a dwell-time of 300 s, is close to a pure creep one for a coarse grain alloy with a fully intergranular fracture surface and secondary cracks initiating at the grain boundaries.

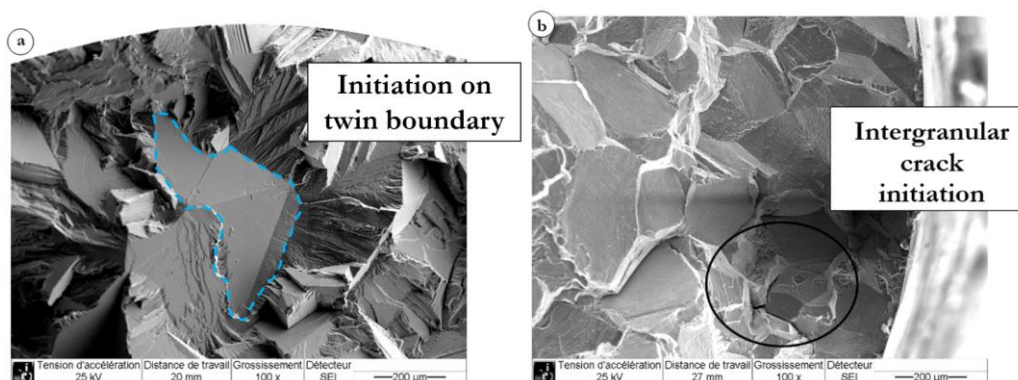


Figure 6. SEM fracture surfaces observations of specimens after creep-fatigue test at 700 °C and $\sigma_{max} = 850$ MPa on the coarse grains microstructure: (a) $\Delta t = 3$ s, (b) $\Delta t = 300$ s.

Comparing the dwell-fatigue behavior to the pure creep one, a striking result is observed: when the maximum applied stress is $\sigma_{max} = 750$ MPa, the addition of the cycling component causes a deterioration of the time to failure, whatever the hold period. As an example, the creep-fatigue life for a 10 s hold period is half that in pure creep (Figure 5a). However, the opposite effect is observed when the maximum applied stress increases to 850 MPa (Figure 5b): for a 10 s dwell time, the creep-fatigue life is 25 h (cumulated time at maximum applied stress), while it is only 20 h in pure creep. The increase in time to failure for long dwell times (300 s and 3600 s) compared to pure creep conditions is even more spectacular at 850 MPa.

These results hence clearly evidence complex creep-fatigue interactions. At 850 MPa, the development of creep damage is dominant and the unloading phases are beneficial to the time to failure while at 750 MPa, the contribution of the fatigue damage (crack initiation and propagation) becomes non-negligible.

4. Discussion

4.1. Deformation and Damage Mechanisms during Creep

The overall creep deformation mechanisms can be deduced from a Norton plot in which the minimum creep strain rate is plotted as a function of the applied stress [14] (Figure 7). At 850 °C, the coarse grains and the single crystals microstructures exhibit similar behaviors. At this temperature, the fine grains' behavior strongly differs from the two other microstructures. The Norton's coefficient n (based of the Norton's law shown in Equation (1)) for the fine grains microstructure is around one, which means that the creep deformation mechanisms are mainly diffusion controlled, while, due to their higher intragranular γ' volume fraction, the coarse grains and single crystals creep behaviors are both at least partly controlled by dislocation creep (Norton's coefficients of five and six respectively).

$$\dot{\epsilon}_{min} = \alpha \left(\frac{\sigma}{\lambda} \right)^n \tag{1}$$

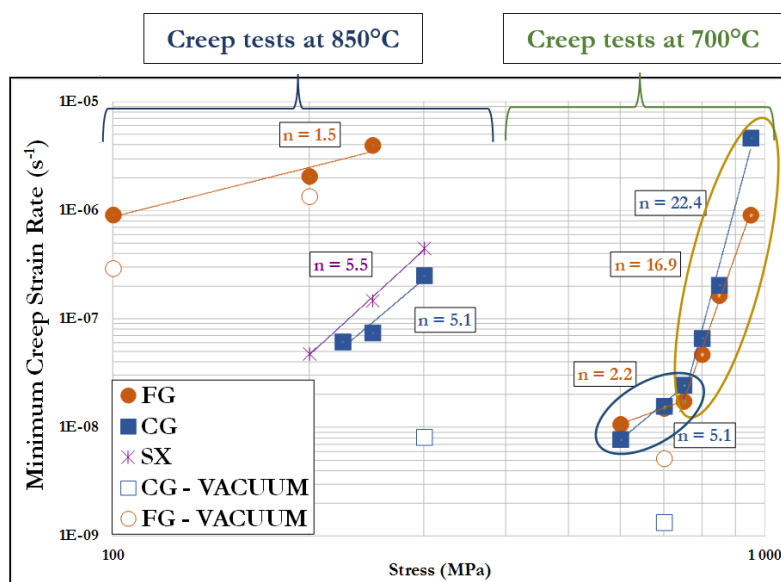


Figure 7. Minimum creep strain rate as a function of the applied stress; n = Norton's coefficient.

SEM observations of crept specimens at 850 °C cut along the tensile direction reveal that the fine grains specimens develop preferential damage in the form of pores along the grain boundaries/primary γ' interfaces (Figure 8a), where vacancies diffusion occurred during the test. Damage is localized at grain boundaries on the coarse grains microstructure (Figure 8b). This indicates that the diffusion mechanisms here are a mix between grain boundary sliding, and vacancies diffusion along grain boundaries. The better creep properties at this high temperature directly result from the decrease in grain boundary density. The grain size is then governing the creep mechanisms under these conditions, up to a threshold grain size. When this threshold is reached, the dislocations motion in the matrix becomes dominant, explaining the close properties between the single crystals and the coarse grains properties at 850 °C. One would also expect a non-negligible contribution of the intragranular γ' volume fraction, this one being close to 32% in single crystalline and coarse grain samples, while it is in the order of 25% in fine grain samples.

Fracture surface observations of the crept specimens at 850 °C confirm the intergranular character of the failure, as we can see in Figure 9.

On the other hand, tests performed at 700 °C on both coarse and fine grains microstructures revealed very similar creep performances. Between 750 MPa and 850 MPa, both microstructures show close creep behaviors, with Norton's coefficients higher than sixteen, leading to a dislocation creep type, while their creep behaviors start to differ below 750 MPa, and their Norton's coefficients are five and two for the coarse grains and fine grains microstructures, respectively. Thus, creep deformation mechanisms below 750 MPa for both microstructures at 700 °C seem to be both diffusion/dislocation controlled for the coarse grains microstructures, and mainly diffusion controlled for the fine grains one.

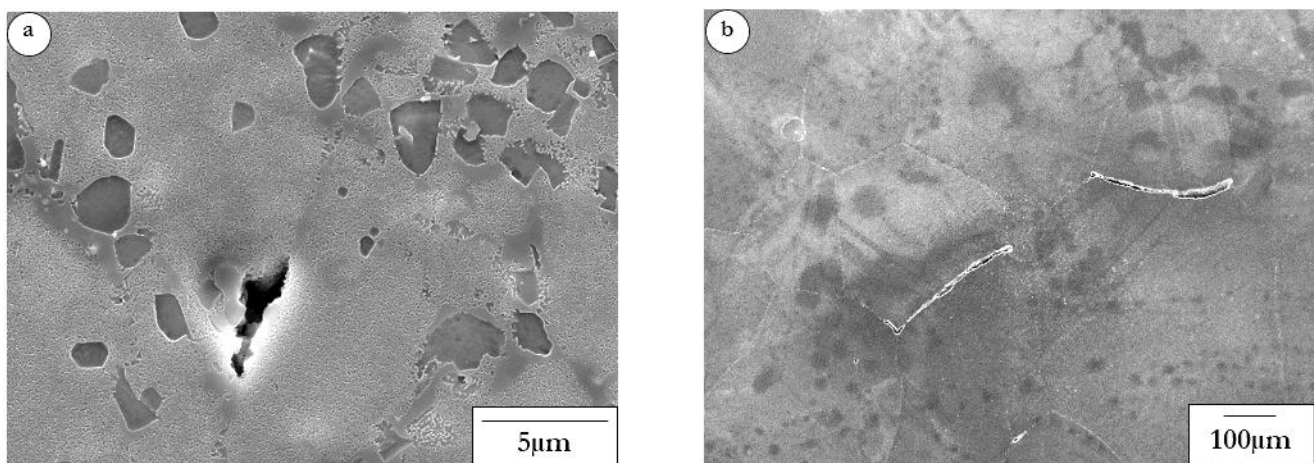


Figure 8. Post-Mortem longitudinal observations: (a) Fine grains microstructure, 850 °C/250 MPa; (b) Coarse grains microstructure, 850 °C/250 MPa.

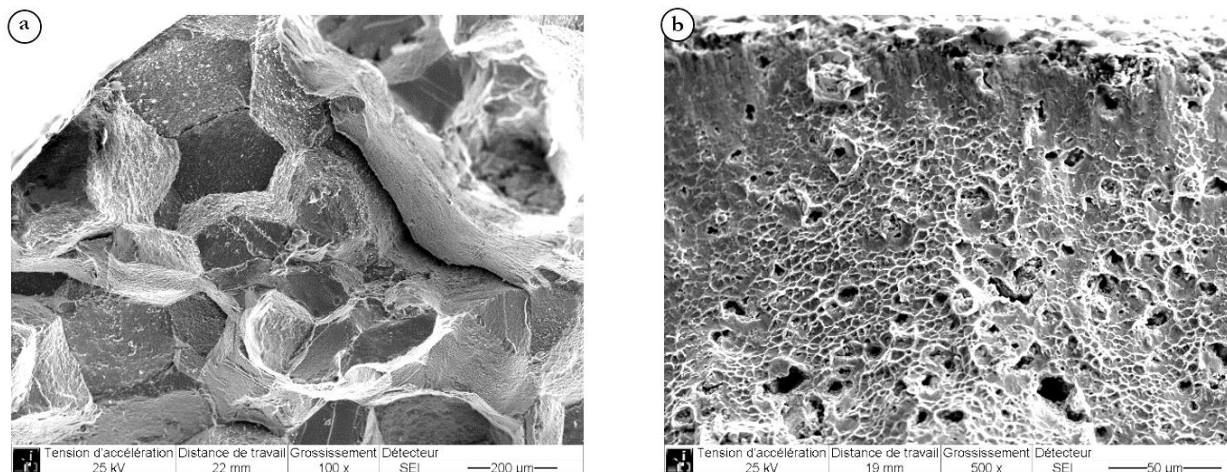


Figure 9. SEM fracture surface observations of crept specimens at 850 °C: (a) Coarse grains microstructure, 850 °C/250 MPa; (b) Fine grains microstructure, 850 °C/200 MPa.

Because the grain size has no impact on the creep properties at 700 °C above 750 MPa, another parameter is then creep-rate controlling. It has already been shown [12,15–17] that at this temperature, the γ' size and distribution are the creep-controlling mechanisms. In this case, both microstructures possess nearly the same secondary γ' size (Figure 1), which could explain why their creep properties are very similar [13].

Thus the threshold stress suggested by the creep life dependence to the applied stress at 700 °C (Figure 4a) is confirmed here by investigating the minimum creep strain rates. The presence of such threshold stress has already been evidenced in other superalloys [18–21], and also suggests that the creep deformation mechanisms at higher stresses are governed by a regime where the dislocations shear the γ' precipitates, whereas dislocation climb is often the rate limiting deformation mechanism under this threshold stress.

Fracture surface observations of crept specimens do not show any evidence of this change in creep deformation mechanisms. In Figure 10, intergranular fracture surfaces are observed for the coarse grains microstructure at 700 °C both at 600 MPa (Figure 10a) and at 850 MPa (Figure 10b).

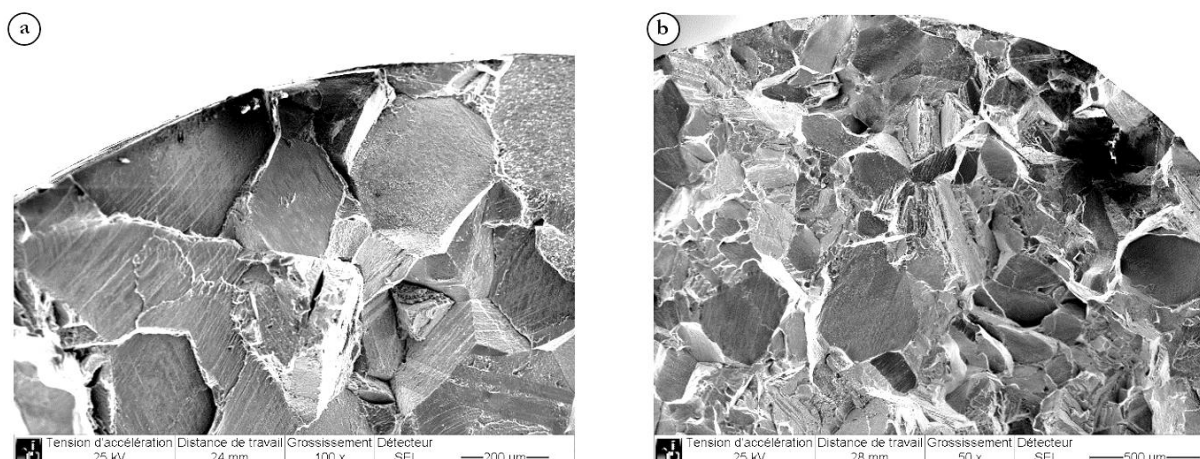


Figure 10. SEM fracture surface observations of crept specimens at 700 °C: coarse grains microstructure; (a) 600 MPa, (b) 850 MPa.

Post-mortem observations along longitudinal cuts of crept specimens at 700 °C, with an applied stress higher than 750 MPa show a strong dislocation activity through γ' precipitates shearing (Figure 11). Further TEM observations would be necessary to confirm the differences in deformation mechanisms below and above this stress threshold. Moreover, additional experiments under vacuum would be required to check if the minimum strain rate dependence to the applied stress observed under air conditions at 700 °C is also sensitive to the environment, as one would expect based on the first results under vacuum shown in Figure 7.

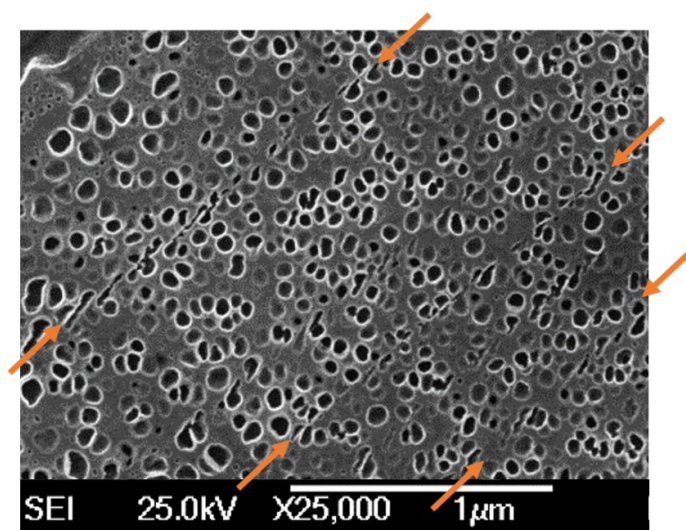


Figure 11. Post-mortem observations on longitudinal cut from crept specimen at 700 °C, fine grains microstructure, 700 °C/800 MPa. Arrows indicate shearing mechanisms.

4.2. Deformation and Damage Mechanisms during Dwell-Fatigue Loading at 700 °C

To understand the differences between dwell-fatigue and pure creep behavior as a function of the maximum applied stress, fracture surface analyses of tested specimens were done on samples tested with $\sigma_{\max} = 750$ MPa and $\sigma_{\max} = 850$ MPa, with the same dwell time: 10 s (Figure 12).

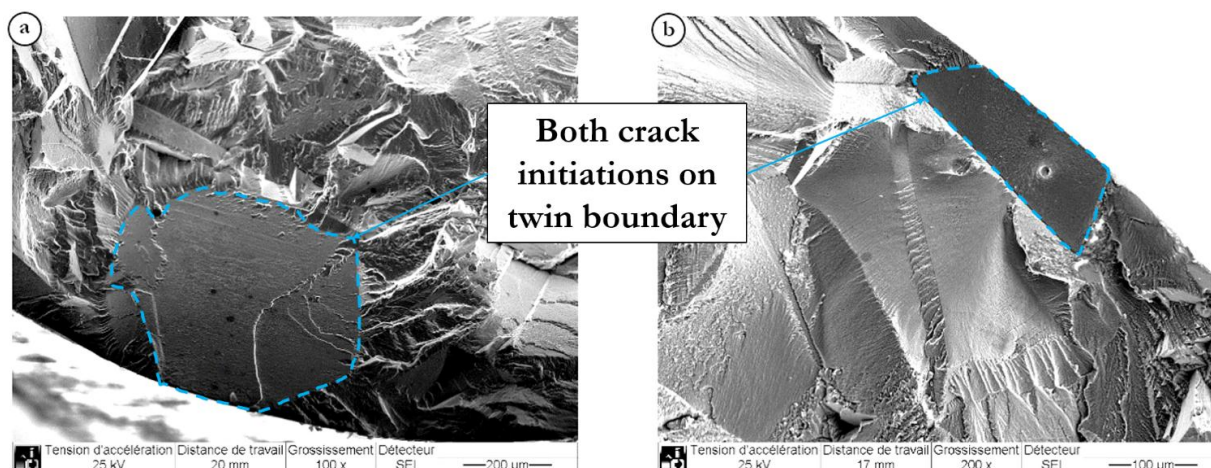


Figure 12. Fracture surface observations of creep-fatigue specimens: coarse grains microstructure, 700 °C— $\Delta t = 10$ s; (a) $\sigma_{\max} = 750$ MPa; (b) $\sigma_{\max} = 850$ MPa.

Both fracture surfaces exhibit similar features, with an initiation site at twin boundaries.

Closer observations of longitudinal sections of the specimens are needed to get a better understanding of this dependence on the applied stress. However, one assumption can be made. Indeed, it has been shown previously in this paper that, for the coarse grains microstructure, at 700 °C in pure creep, a change in creep deformation mechanism occurs around 750 MPa. A dwell-fatigue test, for a given hold period can be seen as a pure creep test with periodic unloading phases. In that case, the dislocation's recovery processes may occur during these unloading phases.

As a result, the change of behavior observed in creep-fatigue when decreasing the maximum applied stress can be linked to the change in the creep deformation mechanism occurring during pure creep at 700 °C, around 750 MPa, as discussed before.

In creep-fatigue, when the maximum applied stress is 850 MPa (*i.e.*, maximum applied stress/0.2% yield stress ratio ~ 0.96), the deformation during the hold periods is expected to be governed by dislocations shearing. The fact that the creep life at 850 MPa is lower than the creep-fatigue life at the same maximum applied stress indicates that the dislocation recovery processes during the relaxation phases have a beneficial impact on the material properties. Indeed, negative plastic deformation (*i.e.*, plastic deformation toward smaller strains) occurs during unloadings. Such a yielding, appearing progressively in the meantime of dwell-fatigue tests at high applied stresses for long dwell time, clearly indicates a pronounced tension/compression asymmetry and, hence, a Bauehinger effect. The overall plastic strain rate during such tests is then slowed down by the unloading phases.

On the other hand, at 750 MPa (*i.e.*, maximum applied stress/0.2% yield stress ratio ~ 0.85), around the creep threshold stress, the creep-controlling mechanisms should be a mixture between dislocations climbing/bypassing over precipitates and shearing. In these instances, the creep life is higher than the dwell-fatigue life. This suggests that the unloading phases are no longer beneficial. In this case, unloadings do not introduce “negative” yielding at minimum stress and apparent slower plastic strain rates at maximum stress. The stress release phases can then be seen as a cycling component, which can be deleterious for the material compared to pure creep, contributing to fatigue damage.

Firstly, dwell-fatigue tests on the fine grains microstructure were conducted at maximum applied stresses higher than the creep threshold stress (950 MPa and 850 MPa), and around it (750 MPa), for hold periods of 10 s. The results from these tests confirm the trend observed on the coarse grains microstructure: when the maximum applied stress is higher than the creep threshold stress, the unloading phases seem to be beneficial to the overall time to rupture, whereas the opposite effect is encountered at maximum applied stress close to the creep threshold stress (750 MPa) (Figure 13).

More tests at different applied stresses and microstructure investigations are needed to analyze and better understand these first results.

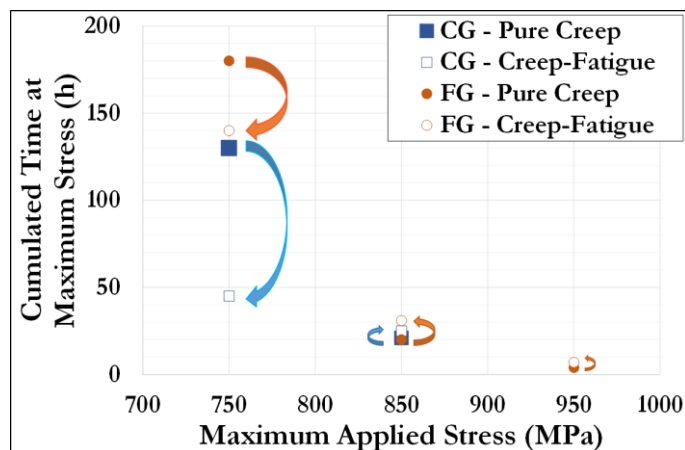


Figure 13. Comparison of pure creep and dwell-fatigue (10 s hold times) time to failure for both microstructures at 700 °C.

5. Conclusions

The viscoplastic behavior of the AD730™ superalloy under pure creep and dwell-fatigue loading has been investigated at 850 °C and 700 °C on three different microstructures in order to investigate the influence of several microstructural parameters. It appears that at 850 °C, if the coarse grains microstructure is more creep resistant than the fine grains one, due to its larger grain size, the single crystalline microstructure is not more creep resistant than the coarse grains one. Hence, the creep behavior mainly depends on the grain size, but also on the intragranular γ' volume fraction. At 700 °C, the creep-controlling parameters depend on the applied stress, for both the fine and the coarse grains microstructure and the grain size is no longer the microstructure controlling parameter. A change in the creep strain rate dependence to the applied stress around 750 MPa has been highlighted, and is assumed to be linked to a change in operative dislocation micromechanisms.

Dwell-fatigue tests performed at 700 °C on both the coarse grains and the fine grains microstructure exhibit a change of influence of the unloading phases on the overall behavior, depending on the maximum applied stress. This suggests that there is a link between the pure creep behaviors at 700 °C and the dwell-fatigue one, with the unloading phases during this type of test playing a prominent role in controlling the time to failure by introducing dislocation recovery mechanisms.

Acknowledgments

The authors would like to thank Aubert & Duval for providing the materials, and for their continuous interest in this study. SAFRAN is gratefully acknowledged for their financial support, and for the continuous collaboration for over 10 years with Institut Pprime on Ni-based superalloys activity.

Author Contributions

Louis Thebaud carried out the experiments and analyzes of the results, with the help of Florence Hamon. Louis Thebaud and Jonathan Cormier prepared and revised the manuscript. Patrick Villechaise and Jonathan Cormier, in collaboration with Alexandre Devaux, Coraline Crozet and Denis B échet from Aubert & Duval, and Jean-Michel Franchet from SAFRAN, initiated and directed

the project. All of the authors helped in the interpretation of the results and followed up on the progress step by step.

Conflicts of Interest

The authors declare no conflict of interest.

References

1. Brooks, J.W.; Bridges, P.J. Metallurgical Stability of Inconel 718. In *Superalloys 1988*, TMS: Warrendale, PA, USA, 1988; pp. 33–42.
2. Devaux, A.; Naz é L.; Molins, R.; Pineau, A.; Organista, A.; Gu édou, J.Y.; Uginet, J.F.; Héritier, P. Gamma double prime precipitation kinetic in Alloy 718. *Mater. Sci. Eng. A* **2008**, *486*, 117–122.
3. Devaux, A.; Georges, E.; Héritier, P. Properties of New C&W Superalloys for High Temperature Disk Applications. In Proceedings of the 7th International Symposium on Superalloy 718 and Derivatives, Pittsburgh, PA, USA, 10–13 October 2010; TMS: Warrendale, PA, USA, 2010; pp. 223–235.
4. Devaux, A.; Georges, E.; Héritier, P. Development of New C & W Superalloys for High Temperature Disk Applications. *Adv. Mater. Res.* **2011**, *278*, 405–410.
5. Devaux, A.; Picqu é B.; Gervais, M.; Georges, E.; Poulain, T.; Héritier, P. AD730™—A New Nickel-Based Superalloy for High Temperature Engine Rotative Parts. In *Superalloys 2012*; TMS: Warrendale, PA, USA, 2012; pp. 911–919.
6. Devaux, A.; Helstroffer, A.; Cormier, J.; Villechaise, P. Effect of Aging Heat-Treatment on Mechanical Properties of AD730™ Superalloy. In Proceedings of the 8th International Symposium on Superalloy 718 and Derivatives, Pittsburgh, PA, USA, 28 September–1 October 2014; TMS: Warrendale, PA, USA, 2014; pp. 521–535.
7. Flageolet, B. Effet du Vieillissement du Superalliage Base Nickel N18 Pour Disques de Turbines sur sa Durabilité en Fatigue et en Fatigue-Fluage à 700 °C. Ph.D. Thesis, École Nationale Supérieure de Mécanique et d’Aérotechnique, Chasseneuil-du-Poitou, France, 2005.
8. Miner, R.; Gayda, J.; Maier, R. Fatigue and creep-fatigue deformation of several nickel-base superalloys at 650 °C. *Metall. Trans. A* **1982**, *13*, 1755–1765.
9. Zrník, J.; Semenak, J.; Vrchovisky, V.; Wangyao, P. Influence of hold period on creep—Fatigue deformation behaviour of nickel base superalloy. *Mater. Sci. Eng. A* **2001**, *319*, 637–642.
10. Billot, T. Comportement et endommagement en fatigue et fatigue-fluage à haute température de différents états microstructuraux du superalliage base-nickel Udimet 720, Ph.D. Thesis, École Nationale Supérieure de Mécanique et d’Aérotechnique, Chasseneuil-du-Poitou, France, 2010.
11. Reed, R.C. *The Superalloys: Fundamentals and Applications*; Cambridge University Press: Cambridge, UK, 2006.
12. Billot, T.; Villechaise, P.; Jouiad, M.; Mendez, J. Creep-fatigue behavior at high temperature of a UDIMET 720 nickel-base superalloy. *Int. J. Fatigue* **2010**, *32*, 824–829.
13. Laurence, A. Impact du sur-vieillissement métallurgique sur le comportement et la durabilité du superalliage base nickel René 65, Ph.D. Thesis, École Nationale Supérieure de Mécanique et d’Aérotechnique, Chasseneuil-du-Poitou, France, 2016.

14. Nabarro, F.; de Villiers, H. *The Physics of Creep*; Taylor & Francis: London, UK, 1995.
15. Laurence, A.; Cormier, J.; Villechaise, P.; Billot, T.; Petinari-sturm, F.; Hantcherli, M.; Momprou, F. Impact of the solution cooling rate and of thermal aging on the creep properties of the new cast&wrought René65 Ni-based superalloy. In Proceedings of the 8th International Symposium on Superalloy 718 and Derivatives, Pittsburgh, PA, USA, 28 September–1 October 2014; TMS: Warrendale, PA, USA, 2014; pp. 333–348.
16. Locq, D.; Caron, P.; Raujol, S.; Pettinari-Sturm, F.; Coujou, A.; Clément, N. On the Role of Tertiary γ' Precipitates in the Creep Behaviour at 700 °C of a PM Disk Superalloy. In *Superalloys 2004*; Green, K.A., Pollock, T.M., Harada, H., Eds.; TMS: Warrendale, PA, USA, 2004; pp. 179–187.
17. Soula, A. Etude de la Déformation Intergranulaire au Cours du Fluage à Haute Température d'un Superalloy à Base de Nickel Polycristallin. Ph.D. Thesis, Institut National Polytechnique de Grenoble, Grenoble, France, 2010.
18. Shewfelt, R.; Brown, L. High-temperature strength of dispersion-hardened single crystals : I. Experimental results. *Philos. Mag.* **1974**, *30*, 1135–1145.
19. McLean, M. On the threshold stress for dislocation creep in particle strengthened alloys. *Acta Metall.* **1985**, *33*, 545–556.
20. Arzt, E.; Wilkinson, D.S. Threshold stresses for dislocation climb over hard particles: The effect of an attractive interaction. *Acta Metall.* **1986**, *34*, 1893–1898.
21. Sinha, N.K. Short strain relaxation/recovery tests for evaluating creep response of nickel-base superalloys like IN-738LC. *J. Mater. Sci. Lett.* **2001**, *20*, 951–953.

© 2015 by the authors; licensee MDPI, Basel, Switzerland. This article is an open access article distributed under the terms and conditions of the Creative Commons Attribution license (<http://creativecommons.org/licenses/by/4.0/>).